Electrochemical Studies to Compare Corrosion Characteristics of Base Metals and Welds of Low Carbon Steels Used in Ship Building Industry

Rishi Pamnani[1*], R.P. George[2], B. Anandkumar[2], M. Vasudevan[2],
U. Kamachi Mudali[2], T. Jayakumar[2]

[1]Prototype Training Centre (Kalpakkam), PO Box 03, Anupuram, Tamil Nadu (India) – 603127
[2] Metallurgy and Materials Group, Indira Gandhi Centre for Atomic Research, Kalpakkam, Tamil Nadu (India) – 603102
*Corresponding author: Rishi Pamnani
E-mail: rishi.rashmi.p@gmail.com , Tel: +91 44 27482024, Fax: +91 44 27482916

Abstract

DMR-249A is a low carbon High Strength Low Alloy (HSLA) steel, with micro-alloying additions of V, Nb and Ti, and has predominantly ferritic microstructure, with pearlite less than 10% by volume. For this structural grade steel used in the construction of the hulls of various vessels, the deterioration of structural strength and structural integrity is a major factor in assets management. This paper discusses comparison of electrochemical properties of both DMR 249A steel and the welded butt joints fabricated with four different welding processes: Manual process - Shielded Metal Arc Welding (SMAW) and Automatic processes - Submerged Arc Welding (SAW), Flux Cored Arc Welding (FCAW) and Activated Flux Tungsten Inert Gas Welding (A-TIG). The microstructures revealed transformation of fine grained equiaxed ferrite structure of DMR 249A to grain boundary ferrite, widmanstatten ferrite, acicular ferrite, polygonal ferrite and microphases in weld metal. The difference in OCP and corrosion rate observed in the base metal and the four different weld joints was also negligible. The base metal (DMR 249A steel) and all weld joints demonstrated similar trends of corrosion within acceptable scatter band establishing that the welding process has not deteriorated the corrosion properties of the base metal. DMR 249A steel was compared with other commercial ship building steels (ABA and D40S) of Russian origin. The corrosion characteristics of DMR 249A with ABA and D40S steels show comparable and analogous trends and extent of corrosion.

Key Words*: Naval Steel (DMR 249A-HSLA), Corrosion, Anodic Polarisation, Tafel Plot, Arc Welding Joints*

Introduction

The shipping construction, offshore and land-based structures use High Strength Low Alloy (HSLA) steel. HSLA steel relates to equiaxed fine grain ferritic steel with good weldability and yield strength of greater than 355 N/mm^2. They are generally Mn alloy grades with approximately 0.2%C and grain-refining elements, such as V, Nb, and Ti. With enhanced resistance to brittle fracture, required yield strength levels are obtained with alloying elements such as Si, Ni, Cu, Cr, and Mo etc. Various low carbon steels (0.04-0.2% C) like HSLA 65, 80, 90, 100, AH 36 etc. have been commercially used as ship

structural steels. The heavy structures require joining of plates using welding by different welding processes [1-3]. DMR-249A is a low carbon HSLA steel, with micro-alloying additions of V, Nb and Ti. The steel has predominantly ferritic microstructure, with pearlite less than 10% by volume [4-5]. This structural grade steel is used for the construction of the hulls of various vessels with specific weight and resilience qualities.

For naval structural material, the deterioration of structural strength and structural integrity is a major factor in assets management. This type of deterioration is influenced by the loss of section thickness for structural elements and by the potential for loss of integrity through corrosion; specially, where protective measures such as paint coatings, galvanizing and cathodic protection can be ineffective. Various studies have been carried out to understand stress corrosion cracking, hydrogen induced cracking, microorganism induced corrosion, pitting, crevice and general corrosion behaviour of base metal and weld joints for the HSLAs [6-8]. A number of studies have been carried out to explain the extent of deterioration caused by pitting corrosion [9–14]. The corrosion processes that occur are usually a result of anodic currents. Information on corrosion rates, passivity and pitting tendencies can be obtained by measurements of current-potential relations under carefully controlled conditions. The specimen potential is scanned slowly towards positive current and therefore acts as an anode such that it corrodes or forms an oxide coating. These measurements are used to determine corrosion characteristics of a material in aqueous environments.

This paper proposes comparison of electrochemical properties of base metal (DMR 249A-HSLA) and welded butt joints fabricated with four different welding processes: Manual process - Shielded Metal Arc Welding (SMAW) and Automatic processes - Submerged Arc Welding (SAW), Flux Cored Arc Welding (FCAW) and Activated Flux Tungsten Inert Gas Welding (A-TIG) by conducting potentiodynamic anodic polarization studies.

ABA and D40S steels are conventional commercial ship building materials and experiments were carried out with base material samples of ABA and D40S steels for comparing and understanding corrosion behavior of DMR 249A steel.

Pitting characteristics were compared using optical microscopy. Microscopic analysis was done using SEM to get more insight into mechanism of corrosion resistance.

Experimental Details

Specimen Preparation

For each weld joint, two plates of dimensions 300x120x10 mm^3 were used. The material composition of the plates and welding parameters used in this study are given in Tables 1 and 2 respectively. After carrying out the weld joint edge preparation (Square Butt for A-TIG and 70° V-Grove for SMAW/SAW/FCAW), plates were welded to make a weld joint of 300x240x10 mm^3 . Welded plates were cut to fabricate five corrosion test specimens of 60x20x10 mm^3, one each for SMAW, SAW, FCAW, A-TIG and Base Metal. Two specimens of 20x20 mm^2 sizes were fabricated from 6 mm and 16 mm plates of ABA and D40S sheets respectively. All the seven samples were polished from 80 to 2400 grit SiC papers, followed by alumina (sizes 5 μm and 1 μm) suspension to obtain mirror finish. The polished specimens were thoroughly degreased by ultrasonic cleaning in acetone.

Table 1 Chemical Composition (wt.%) of Materials:

DMR 249A

C	S	P	Mn	Si	Al	Ni	Nb	V	Ti	Cu/Cr	N_2(ppm)	Fe
0.09	0.006	0.14	1.14	0.18	0.026	0.62	0.039	0.02	0.019	<0.020	56	Bal.

ABA

C	S	P	Mn	Si	Al	Ni	Nb	V	Ti	Cu/Cr	N_2(ppm)	Fe
0.09	0.008	0.13	1.54	0.22	0.024	0.72	0.037	0.18	0.021	<0.020	54	Bal.

D40S

C	S	P	Mn	Si	Al	Ni	Nb	V	Ti	Cu	Cr	N_2(ppm)	Fe
0.11	0.025	0.025	0.7	1.0	0.02	0.7	-	-	-	0.5	0.8	Max 0.008	Bal.

Table 2 Welding Parameters for weld Joints:

Welding Process	Current (A)	Voltage (V)	Speed (mm/sec)	No. of Passes	Heat Input for Weld Length (kJ/mm)	Heat Input for Final Pass (kJ/mm)
A-TIG	270	20	1	2	10.8	5.4
SMAW	120	25	1.5	5	10	2
SAW	485	30	7.5	4	7.76	1.94
FCAW	155	25	3.33	6	7.0	1.16

Microstructure – Weld Joints

The inclusion analysis was carried out on polished specimens with 100x magnification under optical microscope. The etching was done with 2% Nital and microstructure studies were carried out using optical microscope.

Chemical Composition of Welded Joints

The chemical analysis of the weld joints was carried out using Jobin Yuon Make (JY 132F) spurt atomic emission spectrometer. The oxygen and nitrogen percentages were analyzed by using Non Dispersive Infra Red (NDIR) analyzer. Nitrogen % was found to be in the range of 0.002 to 0.005 for all weld joints. Oxygen % was found to be in range of the 0.06 to 0.08 except for A-TIG weld joint with 0.126%. The chemical composition of the weld metal in the case of each weld joint is given in Table 3.

Table 3 Chemical Composition (wt.%) of Weld Joints

Process	C	S	P	Mn	Si	Al	Ni	Nb	V	Ti	Cu/Cr
A-TIG	0.088	0.01	0.016	1.40	0.24	0.03	0.74	0.03	0.02	0.02	<0.02
SMAW	0.053	0.01	0.016	0.84	0.15	0.01	2.27	0.02	0.02	0.02	<0.02
SAW	0.066	0.01	0.013	1.22	0.20	0.01	1.22	0.02	0.02	0.02	<0.02
FCAW	0.050	0.01	0.012	0.63	0.09	0.01	2.06	0.02	0.02	0.02	<0.02

Electrochemical Studies

A conventional three-electrode cell assembly was used for polarization measurements. The potentiodynamic anodic polarization measurements were performed in a flat cell, which has a Teflon O-ring lined hole on one side. The polished surface of the test coupon (the working electrode) was pressed against the O ring, so that the solution in the cell could access the surface inside the O-ring. The reference and counter electrodes are fixed in slots provided on the top of the flat cell. The surface area of the working electrode was 1 cm^2. An Ag/AgCl electrode and a graphite electrode were used as reference and counter electrode respectively. Sea water from Kalpakkam (Bay of Bengal) coast (salinity – 35000 ppm, chloride – 18,981 ppm, sulfate – 2650 ppm, pH – 8.1) [15-16] and fresh water (salinity – 350ppm) were used as the electrolytes.

A computer controlled potentiostat (AUTOLAB PG60, Netherlands) was used to conduct the potentiodynamic polarization experiments. The polarization experiments were carried out in sea water and fresh water as per ASTM standard G5 [17] from OCP to + 1.60 V (SCE) at a scan rate of 10 mV/min (0.167 mV/s). The cathodic and anodic polarization in Tafel region was performed in 3.5% NaCl sea water from -0.3 to -0.9 V (region greater than 200 mV on anodic and cathodic side of the corrosion potential).

After polarization experiments, the specimens were observed under an optical microscope to study the morphology and extent of pitting attack. Further, the specimens were imaged under "SNE3000M Korea" make desktop mini-SEM for detailed pit morphological studies.

Surface Profile Measurements

Talysurf CLI 200, Taylor Hobson Precision, machine was used to carry out surface profile measurements. Data from pitted samples after polarization study was collected one point at a time with each point having a discrete X, Y, Z location with directional resolution of 0.5µm. The profilometry was carried out using laser gauge and CCD sensor.

Results and Discussion

The microstructure study of the base metal DMR 249A and arc welded joints were undertaken using optical microscope. The microstructure of the base metal and weld metals of different arc welded joints at 500x magnification are given in Figure 1.The microstructure of DMR 249A base metal shows predominantly fine grained equiaxed ferrite and some percentage of pearlite of banded type structure. For weld metals, the optical images showed arc welded joints with grain boundary ferrite, widmanstatten ferrite with aligned second phase along with veins of ferrite, acicular ferrite, polygonal ferrite and microphases. The minor changes in percentage of volume fraction of the different ferrites (grain boundary, widmanstatten, acicular and polygonal) was observed in the samples characteristic to the difference in heat input of the various arc welding processes The grain boundary ferrite has equiaxed form or thin veins delineating prior austenite grain boundaries. The side plate widmansttten ferrite is seen as the parallel ferrite laths emanating from prior austenite grain boundaries. The acicular ferrite lies between the bodies of prior austenite grains and is considered a toughening phase due to the interlocking arrangement [1, 18-19]. The performance of weld is strongly influenced by post weld microstructure [20].

The weld microstructure obtained in this study was found to be refined and deleterious mixture of bainite and martensite was not observed.
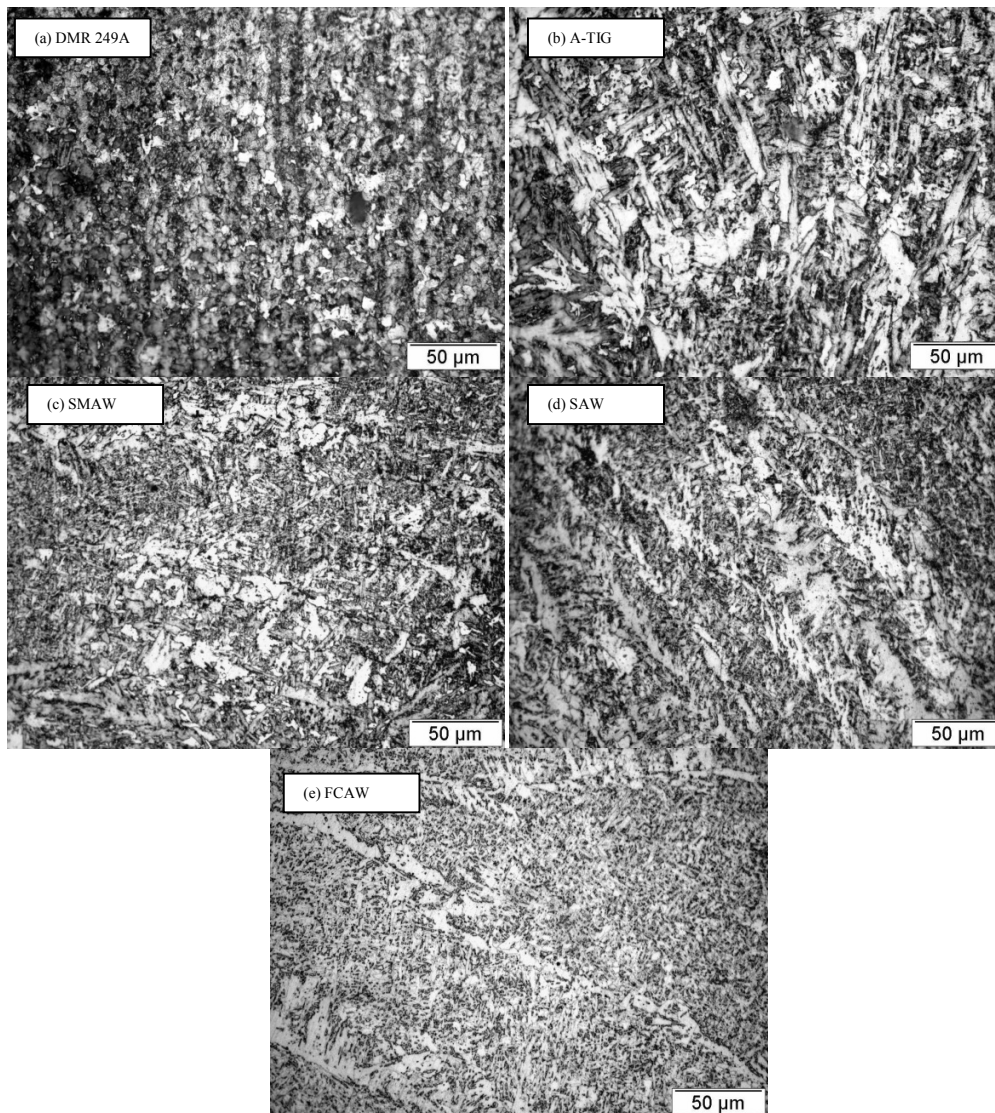

Figure 1 Microstructure Optical Images - BM and Weld Joints (500X)

The anodic polarization graphs for the specimens of DMR 249A base metal and four types of weld metals in sea water and fresh water are given in Figure 2.

The corrosion experiments conducted in sea water (S/W) and fresh water (F/W) as medium seemed to be very similar with virtually indecisive separation in corrosion trends. Though minor differences in OCP and corrosion trends were observed in the base metal and the four weld metals of different welding processes, all specimens demonstrated similar trends within small scatter band. Figure 2 revealed shifting

of corrosion current to higher values and corresponding higher corrosion rates in sea water in comparison to fresh water.

The comparison between DMR 249A, ABA and D40S base metal specimen also showed similar trends of OCP and corrosion trends amongst the three naval structural steels used in this study. The standard characteristic of stainless steel i.e. onset of passivation or metastable pitting was not observed for these HSLA steels. The comparative graphs of DMR 249A, ABA and D40S steels in sea water and fresh water are given in Figure 3.
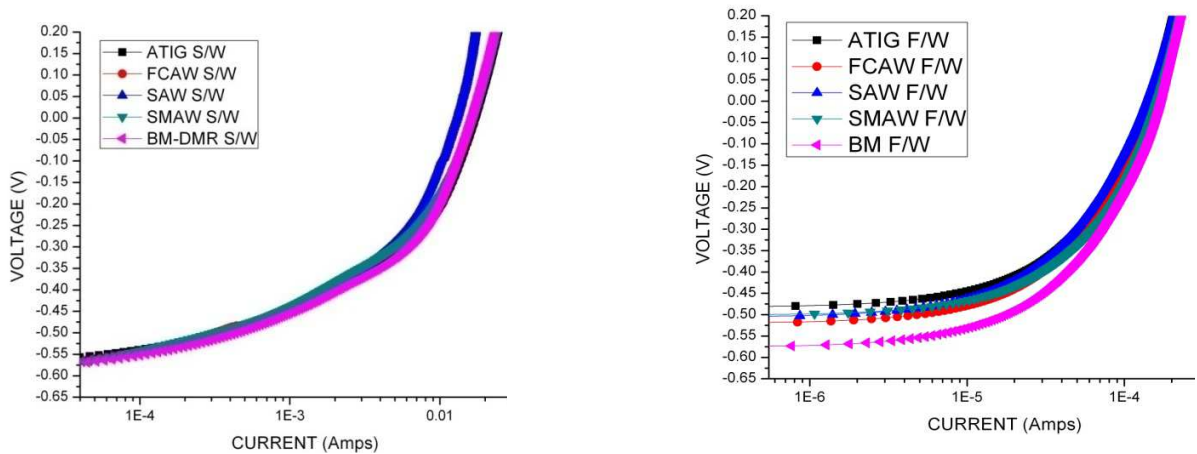
Fig 2(a) Potential-Current Graph-Weld Joints(S/W)   Fig 2(b) Potential-Current Graph-Weld Joints (F/W)
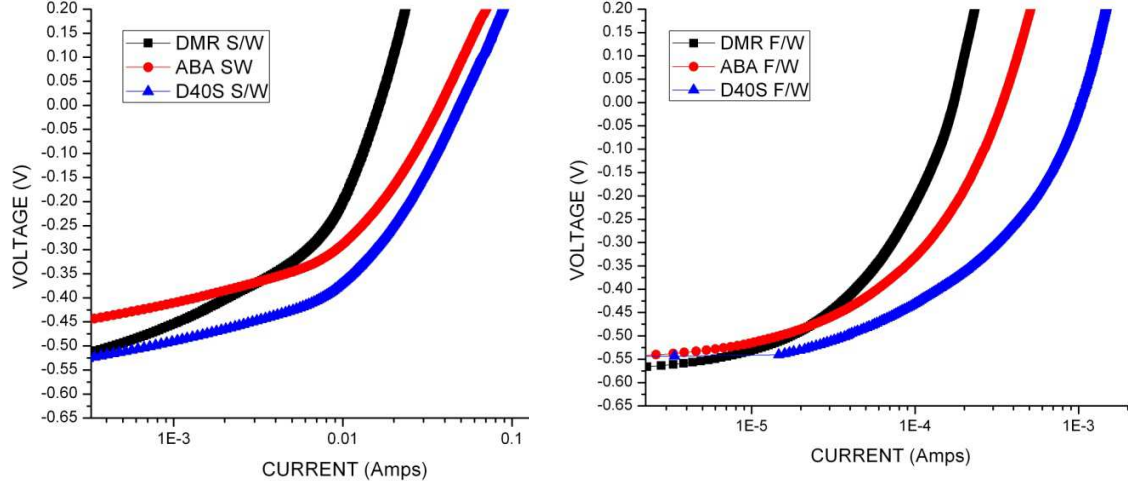
Figure 3(a) Potential- Current Graph- Steels (S/W)   Figure 3(b) Potential- Current Graph- Steels (F/W)

To clarify the differences in corrosion trends, cathodic and anodic polarization studies in the Tafel region were conducted on the specimens in 3.5% NaCl medium to determine the values of corrosion rate, polarization resistance and Tafel constants [21]. The Tafel plots for the four weld metals and the three base metals is given in Figure 4.
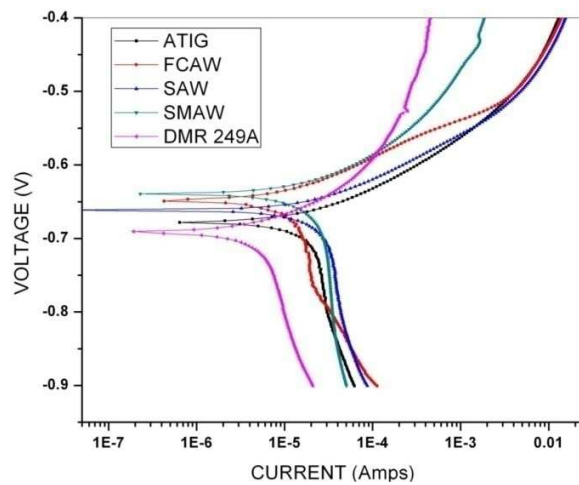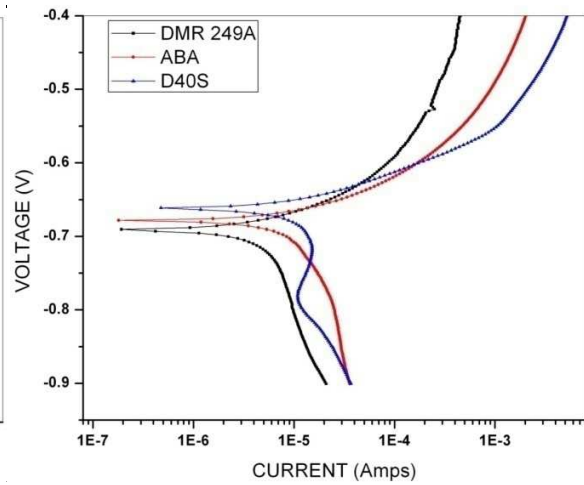
Figure 4(a) Tafel Plot – Weld Joints   Figure 4(b) Tafel Plot – Steels

The corrosion current (I_{corr}) was observed to be in the range of 5.535 E-5 to 9.832 E-6 Amp/cm^2 for the weld metals and 2.975 E-6 to 6.936 E-6 Amp/cm^2 for the base metals. The corrosion potential (E_{corr}) was found to be between -0.702 and -0.647 V for all the tested specimens. The density (ρ) for tested specimens was taken as 7.8 gm/cm^3, equivalent weight of corrosion products as 27.923 gm and corrosion surface area of 1 cm^2 for calculation of corrosion rate in mm per year (CR (mpy)). The corrosion rates of the weld metals varied from 6.483 E-2 to 11.67 E-2 mpy and of base metals from 3.485 E-2 to 8.124 E-2. The comparison of Tafel plot characteristics (cathodic slope b_c, anodic slope b_a and polarization resistance R_p), I_{corr}, E_{corr} and CR for weld joints and base metals is given in Table 4. Though minor differences in Tafel characteristics and corrosion rates were observed in the three base metals and the four different weld metals, all the specimens demonstrated similar trends within the range of 0.03 to 0.1 mpy, with a small scatter band.

Table 4 Comparison of Tafel Plot Characteristics

Specimen	b_c (V/dec)	b_a (V/dec)	R_p (E+2 Ω)	I_{corr} (E-6 Amp/cm^2)	E_{corr} (mV)	CR (E-2 mpy)
Weld Joints						
A-TIG	0.046	0.055	1.132	9.832	-659	10.31
FCAW	0.053	0.054	2.21	5.535	-657	6.482
SAW	0.044	0.055	1.046	9.967	-671	11.67
SMAW	0.062	0.058	1.88	8.296	-639	9.718
Base Metal Steels						
DMR 249A	0.080	0.063	7.393	2.975	-692	3.485
ABA	0.187	0.055	6.46	6.936	-678	8.124
D40S	0.059	0.054	2.031	6.235	-671	7.303

Many corrosion studies have established that inferior corrosion resistance for weld metal as compared to base metal is due to segregation effect [22-25]. The similar corrosion characteristics observed in DMR 249A and weld metals of four different arc welded joints can be attributed to low Chromium content in the base metal (Tables 1&3). Due to the low Cr content, the segregation effect does not cause much of difference in corrosion properties of the base metal and different weld metals.

Earlier research work has established the effect of composition and alloying elements on corrosion behavior of this type of steel [26-30]. The studies have established the detrimental effect of carbon and beneficial effect of Nickel in steel. The marginal increase of Ni content and decrease of C in weld metals of DMR 249A arc weld joints (Tables 1&3) may have also contributed to prevent any deterioration of corrosion in weld metal specimens.

DMR 249A and ABA steels have similar composition. In comparison to DMR 249A and ABA steels, D40S steel has higher carbon and absence of Nb, V and Ti. However, significant amounts of Cu and Cr are present and would have compensated the detrimental effect of higher carbon content [31-32]

The pictures of specimen used post anodic polarization experiments in fresh water and sea water are given in Figure 5. The specimens used for ABA and D40S anodic polarization studies are shown in Figure 6.

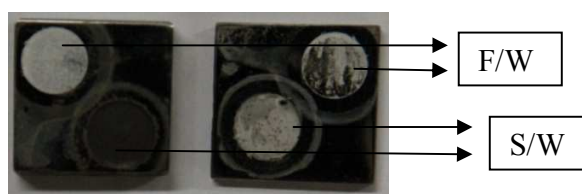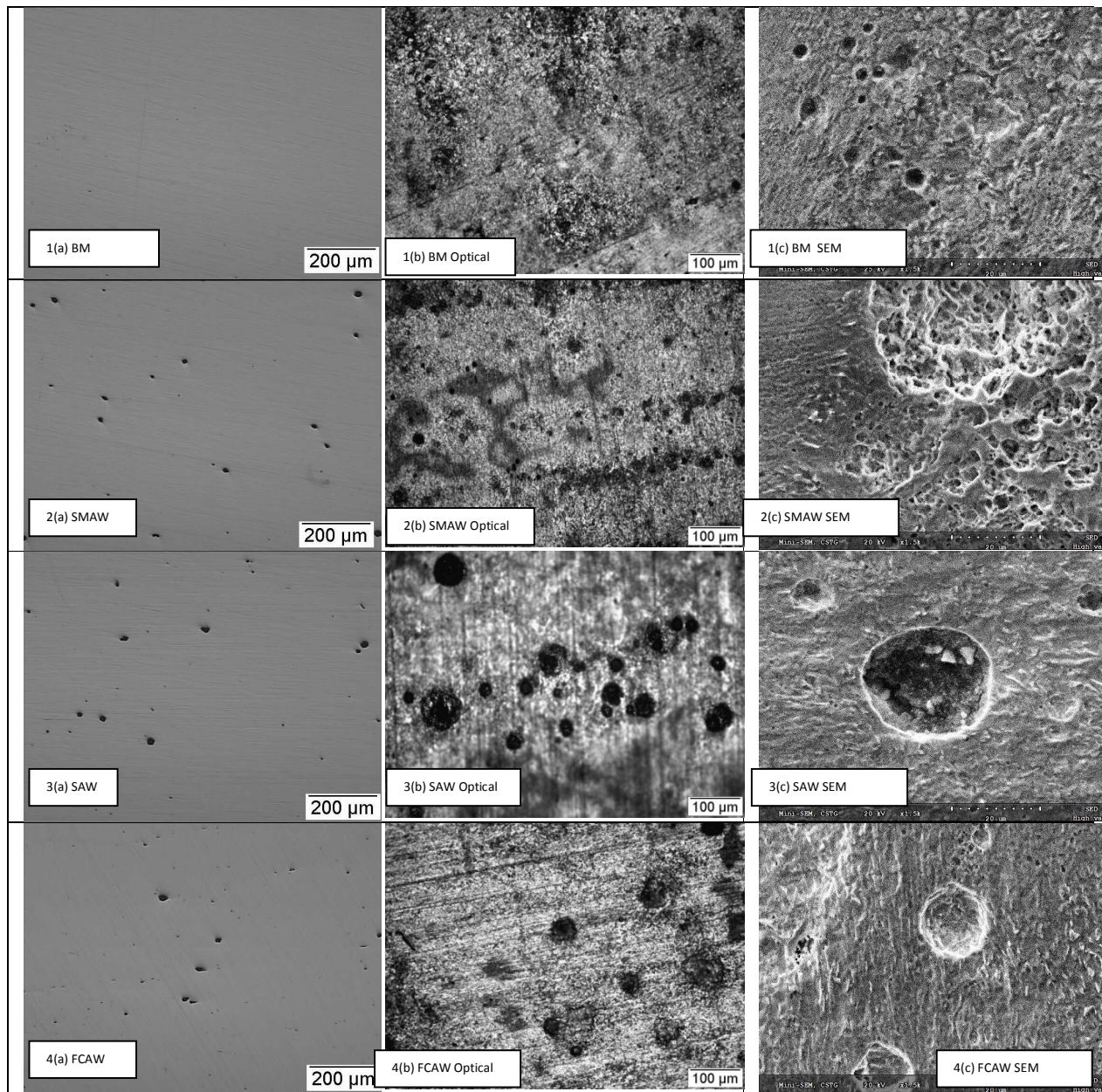Figure 5 BM, SMAW, SAW, FCAW and ATIG-S/W Polarised Samples

Figure 6 D40S and ABA S/W and F/W Specimen

Though the electrochemical polarisation studies showed similar behaviour for DMR 249A base metal and weld metals of arc weld joints, the optical microscopy and SEM observations showed different forms of pitting morphology for the specimens. The base material showed general uniform attack all around the surface with a few pits of excessive depths. A-TIG and SMAW weld joint specimens showed groups of shallow pits with small diameters which can be attributed to small inclusions in the weld metal. FCAW and SAW specimens showed shallow pitting with larger diameter which might be due to the presence of bigger inclusions in weld metals, formed due to the use of flux, acting as corrosion initiation sites. This is similar to the observations made in published literature on effects of inclusions as sites for nucleation/inception for corrosion [33-36]. The optical images of the inclusions in base metal and weld metals of arc welded joints are given in Figure 7 (a).

After the polarization experiments, the specimens were examined under optical microscope and scanning electron microscope (SEM). The photos and images of the optical and SEM are given in Figures 7 (b) and 7 (c) respectively.

The optical and SEM images show general corrosion accompanied by pitting in base metal and weld joint specimens. The pits of bigger diameter were observed in weld joints (ATIG and SMAW (30 to 50 μm), whereas pitting observed in base metal (4 to 12 μm) was of least diameter amongst all the specimens.

1(a) BM   200 μm   1(b) BM Optical   100 μm   1(c) BM SEM

2(a) SMAW   200 μm   2(b) SMAW Optical   100 μm   2(c) SMAW SEM

3(a) SAW   200 μm   3(b) SAW Optical   100 μm   3(c) SAW SEM

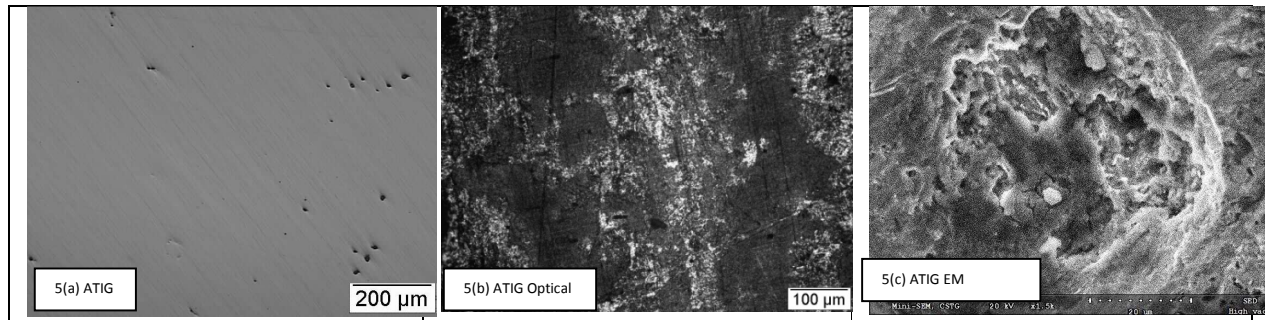4(a) FCAW   200 μm   4(b) FCAW Optical   100 μm   4(c) FCAW SEM

Fig 7- 1. BM (a) As Polished Incusion (100x) (b) Optical (200x) and (c) SEM 1500x
2. SMAW (a) As Polished Incusion (100x) (b) Optical (200x) and (c) SEM 1500x
3. SAW (a) As Polished Incusion (100x) (b) Optical (200x) and (c) SEM 1500x
4. FCAW (a) As Polished Incusion (100x) (b) Optical (200x) and (c) SEM 1500x
5. ATIG (a) As Polished Incusion (100x) (b) Optical (200x) and (c) SEM 1500x

Conclusions

(a)　　　Comparative study to analyze the effect of arc welding methods on corrosion characteristics of DMR 249A steel base metal and weld metals was carried out in sea water and fresh water.

(b)　　　The base metal and weld metals of arc welded joints displayed similar corrosion characteristics for general and pitting corrosion in sea water and fresh water. It was concluded that the qualified arc welding processes did not deteriorate the corrosion characteristics of the base metal, DMR 249A.

(c)　　　The pitting diameter was observed to be smaller for base metal and bigger for weld specimen.

(d)　　　The experiments for corrosion characteristics of DMR 249A with ABA and D40S steel showed comparable trends and similar extent of corrosion in these HSLA steels being used for shipbuilding.

Acknowledgement

References:-

[1] Welding Metallurgy, Kou S, *Willey-Interscience*, 397, 2003.

[2] 'Implementation of HSLA-100 Steel in Aircraft Carrier Construction-The National Shipbuilding Research Program', Christien JP and Warren JL, *Ship Building Production Symposium*, Virginia; 18, pp 1-9, 1993.

[3] 'Status and Prospects of Shipbuilding and Its Weldability', Komizo Yu-Ichi., *Transactions of JWRI*, 36, 1, 2007.

[4] 'Development of Speciality Low Alloy Steels', *International Conference on Metals and Alloys: Past, Present and Future*, pp. 17, 2007.

[5] 'Production of DMR 249A Steel at SAIL, Bokaro Steel Plant', Subrata Mallik, Biswasi Sunita Minz and Basudev Mishra:, *Materials Science Forum, 710, pp 149-154, 2012.*

[6] 'Investigation on Stress Corrosion Cracking Behavior of Welded High Strength Low Alloy Steel in Seawater Containing Various Dissolved Oxygen Concentrations', Huixia Zhang et.al., *Int. J. Electrochem*. Sci., 8 , pp 1262 – 1273, 2013.

[7] 'Hydrogen Degradation of High-Strength Steels', J. Ćwiek, *JAMME*, 37, 2, 2009.

[8] 'Effect of Oxygen and Biofilms on Crevice Corrosion of UNS S31803 and UNS N08825 in Natural Seawater', Laura L. Machuca et.al, *Corrosion Science*, 67, 242-255, 2013.

[9] 'Key issues related to modeling of internal corrosion of oil and gas pipelines – A review', S. Nesic, *Corros. Sci*, 49, pp 4308–4338, 2007.

[10] 'CO$_2$ Corrosion Control in the Oil and Gas Production; Design Considerations', M. Kermani, L. Smith, , *The Institute of Materials*, London, first ed., 1997.

[11] 'Pitting Corrosion of Mild Steel in CO$_2$ Containing NaCl Brine', Z. Xia, K. Chou, Z. Smialowska, *Corrosion*, 45, pp 636–642, 1989.

[12] 'Electrochemical Evaluation of the Corrosion Behaviour of API-X100 Pipeline Steel in Aerated Bicarbonate Solutions', F.F. Eliyan et al., , *Corrosion Science*, 58, pp 181–191, 2012.

[13] 'Corrosion Behaviour of Nano Structured Sol-Gel Alumina Coated 9Cr–1Mo Ferritic Steel in Chloride Bearing Environments', G. Ruhi, O.P. Modi, I.B. Singh, *Surface & Coatings Technology, 204 , pp359–365, 2009.

[14] 'A Comparison Between FSW and TIG Welding Techniques: Modifications of Microstructure and Pitting Corrosion Resistance in AA 2024-T3 Butt Joints A. Squillace', A. De Fenzo, G. Giorleo, F. Bellucci, *Journal of Materials Processing Technology* ,152, pp 97–105, 2004

[15], 'Desalination of Seawater Using Nuclear Heat', M.S. Hanra, *Desalination*, 132, pp263- 268, 2000.

[16] 'Studies on Breakdown of Passivity of Titanium Covered with in Vitro Biofilms', B. Anandkumar, Nanda Gopala Krishna, R.P. George, N. Parvathavarthini and U. Kamachi Mudali, *Journal of Corrosion Science and Engineering*, 16, 26,2013.

[17] 'Standard Reference Test Method for Making Potentiostatic and Potentiodynamic Anodic Polarization Measurements',.*ASTM G5-94(2011)e1*:

[18] 'Corrosion Fatigue Behavior of Submerged Arc Welded High Strength Steel Used in Naval Structures', H. Das and T. K. Pal, *Indian Welding J* , 45,2, pp 40-51, 2012

[19] 'Microstructural Development in Mild and Low-Alloy Steel Weld Metals', Grong O and Matlock DK, *International Metals Reviews*, 31,1, pp 27-48,1986.

[20] 'Microstructure Properties Correlation in Fiber Laser Welding of Dual Phase and HSLA Steels', Saha DC et al. *Materials Sciences and Engineering A* ,607,445-453,2014

[21] 'The Polarization Resistance Technique for Measuring Corrosion Currents', Fontana MG, Staehle RW, Mansfeld F, Advances in Corrosion Science and Technology, 6, Plenum Press, 1976.

[22] 'Corrosion Behaviour of Welded Stainless Steel', Gooch TG, *J. Welding, Welding Research, AWS*, 135-154, 1996.

[23] 'Pitting and Stress Corrosion Cracking Behaviour in Welded Austenetic Stainless Steel', Lu BT et.al, *Electrochemica Acta*, 50, 6, pp 1391-1403, 2005.

[24] 'Effect of TIG welding on Corrosion Behaviour of 316L Stainless Steel', Dadfar M et.al, *Materials Letters*, ,61, 11-12,pp 2343-2346, 2007.

[25] 'Effect of Composition Profiles on Metallurgy and Corrosion Behaviour of Duplex Stainless Steel Weld Metals', Ogawa T and Koseki T, *Welding Research Supplement*, WRC Bulletin, s181-191, 1989.

[26] 'The Corrosion Resistance of Low Alloy Steels', J.C. Hudson, J.F. Stanners,*J. Iron Steel Inst*.,180, pp 271–284, 1955.

[27] 'Corrosion of Metals in Tropical Environments—Part 3—Underwater Corrosion of Ten Structural Steels ',B.W. Forgeson, C.R. Southwell, A.L. Alexander,Corrosion (NACE),16, 3, pp 105–114, 1960.

[28] 'Influence of Alloying Elements on the Marine Corrosion of Low Alloy Steels Determined by Statistical Analysis of Published Literature Data', W.A. Schultze, C.J. van der Wekken, *British Corros. J*, 11, 1,pp 18–24,1976.

[29] 'Verhalten Von Grossbaustahlen in Meerwasser 'J. Petersen, Das, *Werkstoffe und Korrosion* 28, pp 748–754, 1977.

[30] 'Development of High Strength Low Alloy Steels for Marine Applications, Part 1: Results of Long Term Exposure Tests on Commercially Available and Experimental Steels', F. Blekkenhorst, G.M. Ferrari, C.J. van der Wekken, F.P. IJsseling, *Br. Corros. J.* 21,3,pp 163–176, 1986.

[31] 'Effects of Alloying Elements on the Corrosion of Steel in Industrial Atmospheres ', H. E. Townsend ,*Corrosion*, 57, 6, pp. 497-501. *2001*

[32] 'Effects of Cr, Cu, Ni And Ca on the Corrosion Behavior of Low Carbon Steel in Synthetic Fresh Water',Yoon-Seok Choi, Jae-Joo Shim and Jung-Gu Kim ,*Journal of Alloys and Compounds*, 391,1-2, pp162-169, 2005.

[33] 'Corrosion Mechanisms in Theory and Practice', P. Marcus, J. Oudar,Marcel ,*Dekker*, second ,pp. 243-349, 2002.

[34] ' Influence of Microstructure and Non Metallic Inclusions on Sulphide Stress Corrosion Cracking in Low Alloy Steels', V.I. Astafjev, S.V. Artamoshkin, T.V. Tetjueva, *Int. J. Pressure Vessels Piping*, 55, pp 243-250 ,1993.

[35] 'The Influence of Non Metallic Inclusions on the Corrosion Fatigue of Mild Steel', G.P. Ray, R.A. Jarman, J.G.N. Thomas, *Corros. Sci*, 25, pp 171-184, 1985.

[36] 'Effect of Ti-Based Inclusions and Acicular Ferrite on the Corrosion Performance of Multipass Weld Metals' M. Fattahi et al., *Materials Chemistry and Physics*, 146, pp 105-112, 2014.